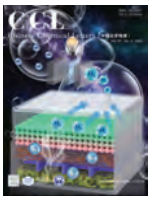
Chinese Chemical Letters 37 (2026) 111668

Contents lists available at ScienceDirect

Chinese Chemical Letters

journal homepage: www.elsevier.com/locate/cclet



Underwater air bubble plasma-activated peroxymonosulfate for sustainable long-term self-purification of wastewater

Xin Li[a], Zhijie Liu[a,*], Hezhi Guo[a], Zekai Zhang[a], Polun Pang[a], Yuting Gao[a], Xiangdong Tan[b]

[a] State Key Laboratory of Electrical Insulation and Power Equipment, Centre for Plasma Biomedicine, School of Electrical Engineering, Xi'an Jiaotong University, Xi'an 710049, China
[b] SINOPEC (Dalian) Research Institute of Petroleum and Petrochemicals Co., Ltd., National Engineering Research Center of Industrial Wastewater Detoxication and Resource Recovery, Dalian 116045, China

ARTICLE INFO

Article history:
Received 11 April 2025
Revised 27 June 2025
Accepted 31 July 2025
Available online 7 August 2025

Keywords:
Underwater bubble plasma activation
Peroxymonosulfate
Self-purification ability
Tetracycline hydrochloride
Wastewater treatment

ABSTRACT

With the continuous detection of new pollutants in the water environment, their potential harm cannot be ignored. In order to explore an effective method to remove contaminants from wastewater, this paper presents an underwater bubble plasma (UBP) activated peroxymonosulfate (PMS) strategy for rapidly degrading the typical emerging contaminant tetracycline hydrochloride (TC) in water. The results indicate that, compared with UBP alone (41.1 %), the UBP-PMS system (98.6 %) exhibits significantly enhanced degradation ability, achieving a 57.5 % increase in TC degradation rate under identical conditions while enabling long-term self-purification of wastewater without energy input within this system. In addition, we studied the effects of initial TC concentration, the type of working gas, the initial pH value of the solution, and the water matrix on the degradation performance of the UBP-PMS system. The anti-interference performance of the UBP-PMS system is proven to be strong, as six inorganic anions (HCO_3^-, CO_3^{2-}, NO_3^-, HPO_4^{2-}, SO_4^{2-} and Cl^-) are added respectively to simulate the actual water environment. The contribution of different reactive species to the degradation process was evaluated qualitatively and quantitatively by electron spin resonance (ESR) and scavenger experiments, of which the largest contribution was $^{\bullet}OH$, followed by $^1O_2$, $ONOOH/O_2^{\bullet-}$, $SO_4^{\bullet-}$ and hydrated electrons. The potential degradation pathways of TC were analyzed, and the toxicity of the degradation intermediates was evaluated by quantitative structure-activity relationship (QSAR) analysis, revealing a gradual reduction in TC toxicity under the co-treatment of UBP-PMS. This study provides a novel activation strategy involving UBP-PMS and provides valuable insights into the degradation properties and mechanisms of emerging pollutants in actual water bodies.

© 2026 Published by Elsevier B.V. on behalf of Chinese Chemical Society and Institute of Materia Medica, Chinese Academy of Medical Sciences.

Antibiotics have been widely used in clinical medicine, animal husbandry, and agriculture due to their excellent ability to control and treat infectious diseases [1,2]. However, the misuse and incorrect discharge of antibiotics have adverse effects on human health and the ecological environment. Tetracycline hydrochloride (TC), a broad-spectrum antibiotic, is currently mainly used in disease control, feed addition, and growth promotion of livestock and poultry [3,4]. It is not only highly ecotoxic and environmentally persistent but also has a high solubility [5,6]. After being metabolized in the body, it is excreted in its original form and is difficult to biodegrade in the environment [1]. Therefore, it is imperative to develop an efficient method for removing TC from water.

Traditional wastewater treatment methods, such as physical adsorption, chemical oxidation, and biological treatment, have limitations such as low degradation efficiency, high operating costs, and secondary pollution [7,8]. Therefore, advanced oxidation processes (AOPs) have been proposed to solve the problems existing in traditional methods. The main feature of AOPs is that they can produce reactive species with strong oxidation properties (mostly $^{\bullet}OH$), and under the reaction conditions of high temperature and pressure, catalysts, *etc.*, the refractory macromolecular organics can be transformed into low toxic or non-toxic small molecular substances [7,9]. In recent years, AOPs based on $SO_4^{\bullet-}$ have attracted more and more attention. Compared with $^{\bullet}OH$, $SO_4^{\bullet-}$ not only has a higher REDOX potential but also can react with refractory organic matter in a wider pH range [10,11].

In general, $SO_4^{\bullet-}$ is mainly produced by peroxymonosulfate (PMS) and persulfate (PS), and due to the asymmetric character-

* Corresponding author.
E-mail address: liuzhijie2010@163.com (Z. Liu).

https://doi.org/10.1016/j.cclet.2025.111668
1001-8417/© 2026 Published by Elsevier B.V. on behalf of Chinese Chemical Society and Institute of Materia Medica, Chinese Academy of Medical Sciences.

istics of PMS, it is more easily activated than PS [10,12]. The common activation methods of PMS mainly include heat, alkali, ultraviolet radiation, transition metal ions and metal oxides, and carbon-based materials activation [12,13]. These activation methods have some problems, such as high energy requirements and secondary pollution. Therefore, it is urgent to find an efficient way to activate PMS. Plasma has attracted more and more attention due to its excellent pollutant removal efficiency and the ability to produce chemicals that contribute to pollutant degradation [14–16]. A variety of physical and chemical effects produced during plasma discharge can effectively activate PMS. However, plasma wastewater treatment is faced with the strong coupling of the gas-liquid interface mass transfer process, which seriously hinders the gas-phase reactive species from entering the liquid phase, resulting in low concentrations of reactive species in contact with pollutants. On this basis, we propose the underwater bubble plasma (UBP), which can be used as an effective mass transfer carrier to carry the gas-phase reactive species into the water and contact with the pollutants, aiming to solve the bottleneck problem of insufficient gas-liquid mass transfer efficiency. Therefore, the process of combining UBP with PMS is a feasible way to improve energy efficiency, achieve a high degradation rate, and reduce environmental pollution. However, the mechanism of UBP activation of PMS is not fully understood, and the influence of different factors on the degradation of pollutants in the UBP-PMS system is not yet known. In addition, the actual wastewater often contains a large number of inorganic ions, and the influence of their presence on the degradation efficiency of pollutants remains to be studied. Most importantly, whether the method combined with UBP and PMS can achieve long-term self-purification without energy input of water bodies, and reduce the toxicity of pollutants, and the reactive species that play a major role in the system also needs to be further explored.

Therefore, the purpose of this study is: (1) To compare the degradation performance of TC in UBP system and UBP-PMS system, to determine whether PMS can be effectively activated by Plasma, and to investigate the long-term self-purification ability of treated water. (2) Analyze the influence of different influencing factors on the degradation rate of TC, and simulate the degradation rate of TC in real water containing a variety of inorganic ions. (3) To study the role of different reactive species in the TC degradation process, speculate the possible TC degradation pathways, and evaluate the toxicity of TC before and after degradation.

Chemicals and reagents, and analysis methods are detailed in Texts S1 and S2 (Supporting information). Batch experiments were carried out in 300 mL beakers containing 200 mL solution. The details of the experimental setup are described in Text S3 (Supporting information). The standard curve of TC is shown in Fig. S1 (Supporting information).

The application of the UBP-PMS system in wastewater containing antibiotics, as demonstrated in Fig. 1a, highlights a significant reduction in both the concentration and toxicity of antibiotics due to the synergistic effects of UBP and PMS. Fig. 1b presents a schematic diagram of TC degradation by the UBP system and the UBP-PMS system, revealing that the discharge process of the combined UBP-PMS system is substantially more vigorous and efficacious.

During the plasma generation process, the flow rate of the working gas greatly affects the residence time of reactive species in the reactor, thereby affecting their contact time with TC [17,18]. As shown in Fig. 1c, during the UBP system, the degradation efficiency of TC increases with the increase of the working gas flow rate. This is because the increase in the working gas flow rate leads to an increase in the supply of oxygen and nitrogen molecules, resulting in an increase in the production of reactive oxygen and nitrogen species (RONS) in the gas phase. Fig. 1d shows the degradation effect of the UBP-PMS system on TC. Compared with the UBP system, the addition of PMS significantly promotes the degradation of TC, because in addition to the RONS generated by the plasma acting on TC, the heat, UV–visible light irradiation and shock wave effects generated by the plasma may help activate PMS to produce $^{\bullet}OH$ and $SO_4^{\bullet-}$, as shown in Eq. 1 [19]. Therefore, there are far more reactive species in the UBP-PMS system than in the UBP system. In the UBP-PMS system, the degradation efficiency of TC first increases and then decreases with the increase of the working gas flow rate, which is attributed to the diffusion limit-driven saturation dynamics. That is to say, the RONS that can interact with TC is limited. When the working gas flow rate exceeds 1 SLM, the residence time of RONS in the discharge area will be shorter, and the degradation of TC will decrease, which in turn destroys the number of RONS that can penetrate the aqueous phase and react with TC [17]. In addition, when the gas flow rate is too high, the small bubbles generated in the device will be combined into large

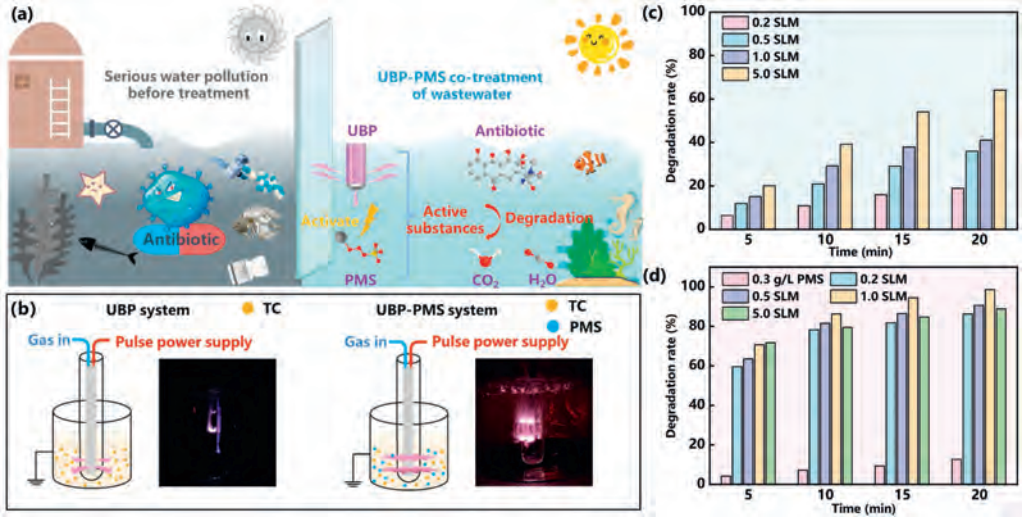


Fig. 1. (a) Application of UBP-PMS system in wastewater containing antibiotics. (b) Schematic diagram of TC degradation in UBP system and UBP-PMS system. (c) TC degradation rate in UBP system. (d) TC degradation rate in UBP-PMS system. Experimental conditions: TC initial concentration = 50 mg/L, PMS concentration = 0.3 g/L, volume: 200 mL, type of working gas = Air.

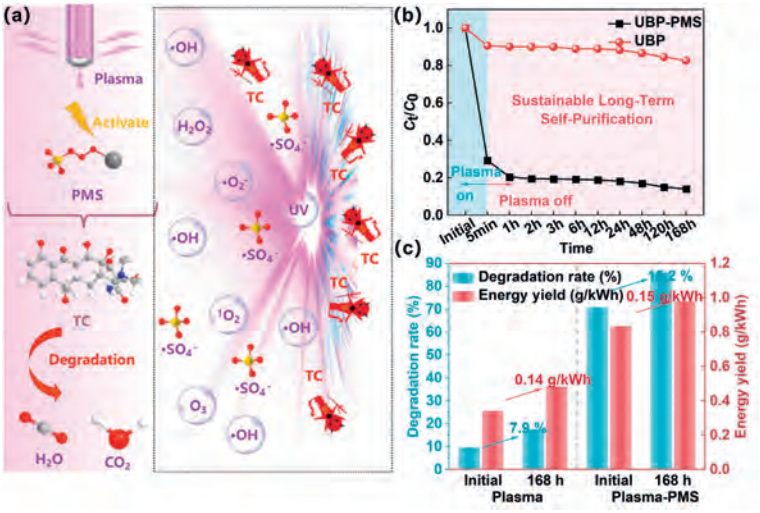


Fig. 2. (a) UBP activation mechanism of PMS. Comparison of TC degradation performance before and after treatment with different systems: (b) C_t/C_0, (c) degradation rate and energy yield. Experimental conditions: TC initial concentration = 50 mg/L, PMS concentration = 0.3 g/L, volume: 200 mL, working gas = 1 SLM air.

bubbles, resulting in the decline of gas-liquid mass transfer efficiency [20]. After 20 min of discharge treatment, when the working gas flow rates were 0.2, 0.5, 1, and 5 SLM, the removal rates of TC in the UBP system reached 18.9 %, 36.0 %, 41.1 %, and 64.1 %, respectively. At the same working gas flow rate, the degradation efficiency of TC by the UBP-PMS system is 86.3 %, 90.6 %, 98.6 %, and 88.8 %, respectively, which is higher than that of the UBP system. In addition, when PMS is treated alone, the removal rate of TC is 12.7 %, which is attributed to PMS's own oxidation ability. As shown above, 1 SLM was selected as the optimal working gas flow rate in subsequent experiments. The kinetic constants and kinetic curves of the UBP and UBP-PMS systems are shown in Fig. S2 (Supporting information). The contrast of absorbance between the two systems at 1 SLM air is shown in Fig. S3 (Supporting information), and the corresponding voltage and current waveforms are shown in Fig. S4 (Supporting information). We compared the degradation results of TC by the UBP-PMS system with those of other techniques. Encouragingly, in the UBP-PMS system, the degradation efficiency of TC after 20 min is higher than that of other systems. The specific data are shown in Table S1 (Supporting information).

$$HSO_5^- \xrightarrow{\text{Plasma}} SO_4^{\bullet-} + {}^\bullet OH \quad (1)$$

Fig. 2a shows the mechanism of UBP activation of PMS. As a new AOP, plasma can generate a large number of reactive species with high REDOX potential and other energies, which can promote the degradation of pollutants [14,21]. In addition, various physical and chemical effects produced by the plasma can activate the PMS to produce $SO_4^{\bullet-}$ with strong oxidation properties. Under the joint action of UBP and PMS, pollutants can achieve efficient degradation. At present, one of the biggest bottlenecks in the large-scale practical application of plasma treatment is energy consumption. How to achieve a high degradation rate and high energy efficiency is the key problem to be solved [8]. As shown in Fig. 2b, when the UBP-PMS system is used to treat TC, the degradation rate is significantly improved, reaching 70.8 % within 5 min, which is significantly higher than that of the UBP system (9.5 %). In addition, as shown in Fig. 2c, the energy efficiency of the UBP-PMS system (0.83 g/kWh) is more than twice that of the UBP system (0.34 g/kWh). Therefore, the addition of PMS can achieve a high degradation rate and high energy efficiency at the same time. In addition, the long-term self-purification ability of the water body is also crucial in practical application. It refers to the ability of the water body to purify and restore water quality through a series of physical, chemical, and biological processes [8]. As shown in Fig. 2c, without input of the energy, the degradation rate and energy efficiency of the UBP system and UBP-PMS system have been improved to a certain extent after 168 h. The degradation rate of the UBP-PMS system has increased from 70.8 % to 86.0 %, and that of the UBP system has only increased by 7.9 %. This shows that the UBP effectively activates PMS to participate in the degradation process of TC. When the plasma is turned off, the oxidation process continues, and reactive species are still produced in the system. This process is conducive to further degradation of residual pollutants in the solution. The long-term self-purification ability of water is very important in practical applications, which can further degrade pollutants without adding additional energy so that the degradation efficiency and energy efficiency have been improved. The UBP-PMS system proposed in this study can realize long-term self-purification of water bodies, which provides a new strategy for the degradation of pollutants in wastewater.

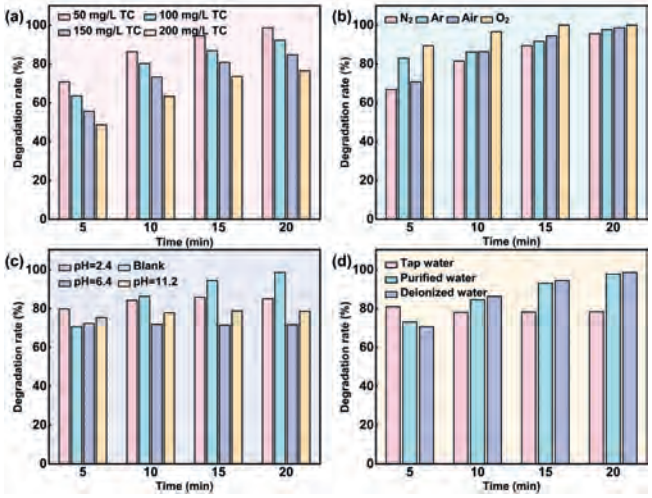


Fig. 3. Factors affecting TC degradation: (a) Initial concentration of TC, (b) the type of working gas, (c) the initial pH value of the solution, (d) the water matrix. Experimental conditions: PMS concentration = 0.3 g/L, volume: 200 mL.

The effects of pollutant concentration, type of working gas, initial pH value of solution, and water matrix on TC degradation rate were investigated, as shown in Fig. 3. The corresponding kinetic

constants and kinetic curves are shown in Fig. S5 (Supporting information). Fig. 3a shows that as the initial concentration of TC increases from 50 mg/L to 200 mg/L, the removal rate of TC decreases from 98.6 % to 76.5 % after 20 min of reaction. This is because the amount of reactive species produced in the same system is determined, and as the TC concentration increases, the competition among TC molecules for the reactive species also increases, so the degradation rate decreases. A large number of studies also show that the increase in pollutant concentration has a great impact on degradation efficiency [18,22].

Fig. 3b shows the degradation rate of TC under different working gases, in which O_2>Air>Ar>N_2. When the working gas is O_2, the reactive oxygen species generated by discharge are the main factors for TC degradation, with $^{\bullet}OH$, O_3, and H_2O_2 playing the main role [23]. Meanwhile, during the discharge process, accompanied by the generation of UV, O_3, and H_2O_2 generates more $^{\bullet}OH$ under its stimulation [23]. When the working gas is air, a large amount of reactive nitrogen species and nitrogen ions (NO_x, $\cdot NO_x$, HONOO, NO_x^-) will be produced in the system. Due to the lower oxidizing ability of reactive nitrogen species compared to reactive oxygen species, the removal rate of TC decreases. In addition, the formation of reactive nitrogen species consumes a certain amount of oxygen, which leads to a decrease in the amount of reactive oxygen species in the system [24]. When Ar is used as the working gas, $^{\bullet}OH$ and H_2O_2 are the main substances for degrading TC. When Ar is excited, it will exist in a metastable state ($Ar(^3P)$), and the high-energy electrons generated by excitation will interact with water molecules to generate $^{\bullet}OH$ and H_2O_2. When N_2 is selected, the degradation effect of TC is the worst, because the content of reactive nitrogen species is too high. The reaction equations involved are in Text S4 (Supporting information).

The initial pH value of the solution can affect the activation of PMS and the existing form of reactive species in aqueous solution. Fig. 3c illustrates the degradation rate of TC in solutions with different initial pH values, demonstrating that suitable acidic conditions are more conducive to the degradation of TC. This may be due to the conversion of part of $SO_4^{\bullet-}$ to $^{\bullet}OH$ under alkaline conditions. The oxidation–reduction potential of $^{\bullet}OH$ (2.7 V under acidic conditions and 1.9 V under alkaline conditions) is lower than $SO_4^{\bullet-}$, so the degradation rate of TC under alkaline conditions is low [8]. But at the same time, it should be noted that in an environment with too strong acidic conditions, acid-catalyzed decomposition of PMS may occur, which will consume PMS without generating free radicals [25]. In general, the degradation of TC can be accelerated by adjusting the initial pH value of the solution in practical applications.

The water matrix is another important factor affecting TC degradation rate. Deionized water, purified water, and tap water were used to evaluate the effect of the water matrix on TC degradation efficiency in the UBP-PMS system. As shown in Fig. 3d, the degradation rate of TC in deionized water and purified water is similar, much higher than that in tap water. This is because there are a large number of ions in tap water, which is not conducive to the generation of plasma and reactive species, so the degradation rate of TC in tap water is low [26].

Natural water has certain ionic strength, and inorganic ions are essential components, which can affect the activation of PMS and the degradation of organic pollutants [27]. To evaluate the effect of inorganic anions on TC degradation, we selected six inorganic anions (HCO_3^-, CO_3^{2-}, NO_3^-, HPO_4^{2-}, SO_4^{2-} and Cl^-) as representatives to study the degradation effect of TC, as shown in Fig. 4. The results showed that these six inorganic anions slowed down the degradation of TC to varying degrees. Among them, HCO_3^-, CO_3^{2-}, HPO_4^{2-}, and Cl^- mainly consume $^{\bullet}OH$ and $SO_4^{\bullet-}$ in the system to reduce the degradation rate of TC, as shown in Eqs. 2–9 [8,28]. As a free radical scavenger, NO_3^- removes part of $SO_4^{\bullet-}$ through

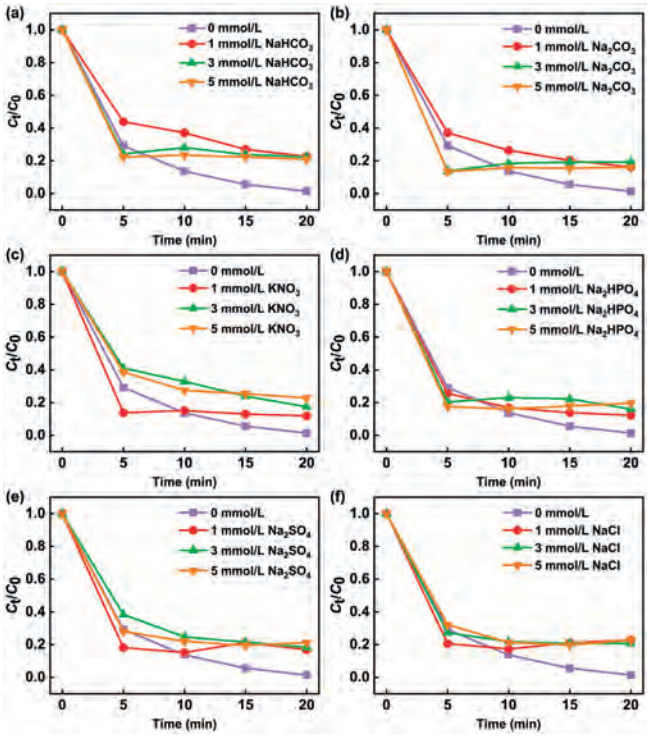


Fig. 4. Inhibitory impact of adding common inorganic anions: (a) HCO_3^-, (b) CO_3^{2-}, (c) NO_3^-, (d) HPO_4^{2-}, (e) SO_4^{2-}; (f) Cl^-. Experimental conditions: TC initial concentration = 50 mg/L, PMS concentration = 0.3 g/L, volume: 200 mL, working gas = 1 SLM air.

Eq. 10, which affects the degradation of TC [29]. SO_4^{2-} as the reaction product after consumption of $SO_4^{\bullet-}$ is not conducive to the conversion of $HSO_5^{\bullet-}$ to $SO_4^{\bullet-}$ so SO_4^{2-} has a certain effect on the degradation of TC [30]. In general, the presence of inorganic anions in the actual water will hinder the degradation of TC to a certain extent, but the degradation rate can still reach >77.0 %, indicating that the UBP-PMS system has a good anti-interference ability.

$$HCO_3^- + {}^{\bullet}OH \rightarrow HCO_3^{\bullet} + OH^- \quad (2)$$

$$HCO_3^- + OS_4^{\bullet-} \rightarrow HCO_3^{\bullet} + SO_4^{2-} \quad (3)$$

$$CO_3^{2-} + {}^{\bullet}OH \rightarrow CO_3^{\bullet-} + OH^- \quad (4)$$

$$CO_3^{2-} + SO_4^{\bullet-} \rightarrow CO_3^{\bullet-} + SO_4^{2-} \quad (5)$$

$$HPO_4^{2-} + {}^{\bullet}OH \rightarrow HPO_4^{\bullet-} + OH^- \quad (6)$$

$$HPO_4^{2-} + SO_4^{\bullet-} \rightarrow HPO_4^{\bullet-} + SO_4^{2-} \quad (7)$$

$$Cl^- + {}^{\bullet}OH \leftrightarrow HClO^{\bullet-} \quad (8)$$

$$Cl^- + SO_4^{\bullet-} \rightarrow Cl^{\bullet} + SO_4^{2-} \quad (9)$$

$$NO_3^- + SO_4^{\bullet-} \rightarrow NO_3^{\bullet} + SO_4^{2-} \quad (10)$$

We used electron spin resonance (ESR) to verify the existence of reactive species in the UBP-PMS system. As shown in Fig. 5a, when the UBP-PMS system is turned on, signals of $^{\bullet}OH$ (1:2:2:1), $SO_4^{\bullet-}$ (1:1:1:1:1:1), ONOOH (1:1:1) and $^1O_2$ (1:1:1) can be detected [31]. When the UBP-PMS system is shut down $^{\bullet}OH$ and $SO_4^{\bullet-}$ signals

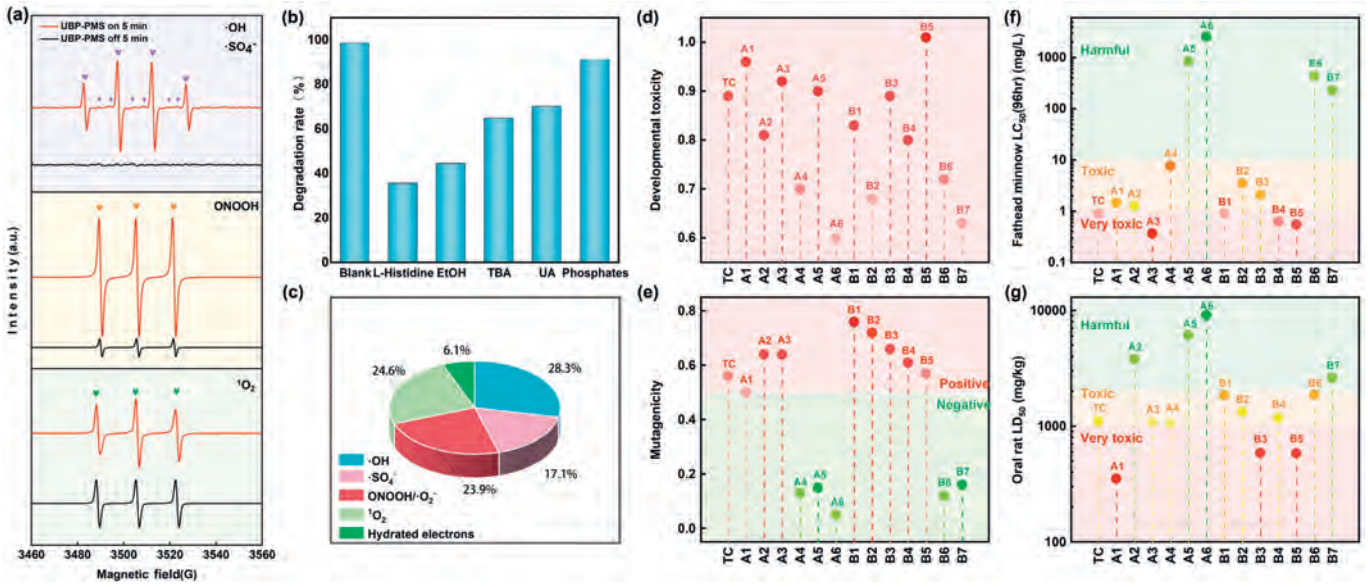


Fig. 5. (a) ESR spectrum, (b) TC degradation rate after addition of scavengers, (c) reactive species contribution proportion. Toxicities of TC and its degradation intermediates: (d) developmental toxicity, (e) mutagenicity, (f) Fathead minnow LC_{50}, (g) oral rat LD_{50}.

disappeared significantly, ONOOH signal weakened significantly, and $^1O_2$ signal also weakened, indicating that after the UBP-PMS system was shut down, the ability to produce reactive species decreased. At this time, the reactive species that can continue to degrade pollutants are mainly $^1O_2$, which is also the reason why the UBP-PMS system can achieve long-term self-purification.

To evaluate the contribution rate of each reactive species to TC degradation, we used the scavenger experiment for calculation. The reactive species quenched by each scavenger are shown in Table S2 [31]. The degradation rate of TC corresponding to the addition of various scavengers is shown in Fig. 5b, and it is observed that the degradation rate of TC decreases to varying degrees. The contribution rate of various reactive species to TC degradation is approximately calculated by Eq. 11, and the contribution rate of various reactive species is normalized [32]. The results are shown in Fig. 5c, and the order is: $^{\bullet}OH > {}^1O_2 > ONOOH/O_2^{\bullet-} > SO_4^{\bullet-} >$ hydrated electrons.

$$CR = \frac{D_{UBP-PMS} - D_S}{D_{UBP-PMS}} \quad (11)$$

where $D_{UBP\text{-}PMS}$ refers to the degradation rate of TC in the UBP-PMS system, and D_S refers to the degradation rate of TC in the system after adding different kinds of scavengers.

The degradation process of TC in the UBP system and UBP-PMS system is studied by LC-MS technology, and the possible degradation paths of TC are speculated. The results of LC-MS are shown in Fig. S6 (Supporting information), and the presumed degradation paths are shown in Fig. S7 (Supporting information). Main degradation intermediates are **A1** (*m/z* 431), **A2** (*m/z* 386), **A3** (*m/z* 370), **A4** (*m/z* 165), **A5** (*m/z* 133), **A6** (*m/z* 119), **B1** (*m/z* 431), **B2** (*m/z* 417), **B3** (*m/z* 388), **B4** (*m/z* 345), **B5** (*m/z* 249), **B6** (*m/z* 173) and **B7** (*m/z* 87). Combined with these detection products and related reports, we inferred the TC degradation path A in the UBP system and the TC degradation path B in the UBP-PMS system. In path A, the addition of $^{\bullet}OH$ group occurs at the C–C double bond position of the TC molecule. Due to the low binding energy of the C–N bond, the amino group is also removed after the two methyl groups centered on the tertiary amine in the TC molecule are continuously attacked [7]. Then, under the attack of different reactive species, **A4** is formed through a series of ring opening and bond-breaking reactions, and **A4** is oxidized into lower molecular weight intermediates **A5**, and **A6**, and then degraded into small molecules such as H_2O and CO_2 [3,33]. In path B, similar to path A, the C–N bond is broken, followed by further demethylation and deamination [34]. Finally, through a series of ring-opening reactions, **B6** and **B7** are formed, and under the impact of $^{\bullet}OH$, $SO_4^{\bullet-}$, $^1O_2$, and $O_2^{\bullet-}$, they are finally mineralized into small molecules such as H_2O and CO_2 [4,35].

Based on the results of liquid chromatograph mass spectrometer (LC-MS), we speculated that there are six degradation intermediates (**A1**-**A6**) in TC degradation path A and seven degradation intermediates (**B1**-**B7**) in TC degradation path B. Degradation of the intermediate information is summarized in Table S3 (Supporting information). Then, the toxicity assessment software tool (T.E.S.T.) was used to evaluate the developmental toxicity, mutagenicity, Fathead minnow LC_{50} (96 h), and oral rat LD_{50} of TC and its degradation intermediates by quantitative structure-activity relationship (QSAR), as shown in Figs. 5d–g [34,36]. In Figs. 5d and e, both TC and its degradation intermediates showed "Developmental toxicant", but the developmental toxicity of most degradation intermediates was reduced, and the mutagenicity became "Negative" (**A4**, **A6**, **B6**, **B7**). Fig. 5f shows that the LC_{50} value of TC is 0.90 mg/L, which is a "Very toxic" substance. The LC_{50} of the degradation intermediates except **A3**, **B4**, and **B5** was higher than that of TC, and the LC_{50} of **A5**, **A6**, **B6**, and **B7** increased sharply with the degradation process, indicating that less toxic intermediates were produced. In Fig. 5g, LD_{50} of TC is shown as a toxic substance, and degradation intermediates **A1**, **B3**, and **B5** are "Very toxic". With the progress of the degradation process, the toxicity is gradually reduced through the fracture of the benzene ring, and some small molecule products are labeled as "Harmful". In general, although the toxicity of some degradation intermediates is greater than TC, with the continuous degradation process, its concentration is far less than TC, so the overall toxicity of TC is gradually reduced during the entire degradation process.

In summary, the performance and mechanism of TC degradation by UBP activated PMS process were thoroughly studied in this study. The results show that UBP can effectively activate PMS, and the degradation rate of TC can reach 98.6 % within 20 min. It is worth noting that when the UBP is turned off, the activated PMS can continue to degrade the TC, thereby improving energy efficiency and achieving long-term self-purification of the wastewa-

ter. The concentration of pollutants, the type of working gas, the initial pH value of the solution, and the water matrix all affect the degradation rate of TC. In addition, the presence of common inorganic anions in the actual water has little influence on the degradation system, and the UBP-PMS system shows good anti-interference ability. In the degradation process, multiple reactive species participate in the degradation of TC and show a synergistic effect. According to the ESR and reactive species scavenging experiments, the contributions of different reactive species are as follows: $^{\bullet}OH > {}^{1}O_2 > ONOOH/O_2^{\bullet-} > SO_4^{\bullet-} >$ hydrated electrons. Finally, two main degradation pathways of TC were speculated and toxicity analysis was conducted. The results showed that the overall toxicity of TC decreased during the degradation process. It can not only achieve high degradation efficiency, but also the activated UBP-PMS system can realize long-term self-purification of wastewater, which provides a practical technical scheme for the efficient degradation of antibiotic wastewater.

Declaration of competing interest

The authors declare that they have no known competing financial interests or personal relationships that could have appeared to influence the work reported in this paper.

CRediT authorship contribution statement

Xin Li: Writing – review & editing, Writing – original draft, Visualization, Investigation. **Zhijie Liu:** Formal analysis, Funding acquisition, Supervision, Writing – review & editing. **Hezhi Guo:** Software. **Zekai Zhang:** Software. **Polun Pang:** Supervision, Methodology. **Yuting Gao:** Supervision, Methodology. **Xiangdong Tan:** Supervision, Methodology.

Acknowledgments

This work was supported by the National Natural Science Foundation of China (No. 12075188), the Natural Science Foundation of Sichuan Province (No. 2024NSFSC0532), the Sichuan Science and Technology Program (No. 2024ZYD0061), Open Project of National & Local Joint Engineering Research Center for Environmental Pollution Control of Petroleum and Petrochemicals (No. 34880000-25-ZC0607-0122), and State Industry-Education Integration Center for Medical Innovations at Xi'an Jiaotong University.

Supplementary materials

Supplementary material associated with this article can be found, in the online version, at doi:10.1016/j.cclet.2025.111668.

References

[1] R. Liang, H. Wu, Z. Hu, et al., Chin. Chem. Lett. 36 (2025) 110136.
[2] X. Zhang, B. Xu, S. Wang, et al., Appl. Catal. B 306 (2022) 121119.
[3] B. Zhang, X. He, C. Yu, et al., Chin. Chem. Lett. 33 (2022) 1337–1342.
[4] Y. Wu, Y. Xu, Y. Zhang, et al., Chin. Chem. Lett. 33 (2022) 2741–2746.
[5] Y. Dai, M. Liu, J. Li, et al., Sep. Sci. Technol. 55 (2019) 1005–1021.
[6] R. Daghrir, P. Drogui, Environ. Chem. Lett. 11 (2013) 209–227.
[7] F. Yang, D. Wang, X. Zhang, et al., Chin. Chem. Lett. 35 (2024) 109599.
[8] L. Liu, J. Zhu, Q. Liu, et al., J. Water Process Eng. 68 (2024) 106541.
[9] J. Wang, S. Wang, Chem. Eng. J. 334 (2018) 1502–1517.
[10] L. Lai, J. Yan, J. Li, et al., Chem. Eng. J. 343 (2018) 676–688.
[11] R. Yuan, S.N. Ramjaun, Z. Wang, et al., J. Hazard. Mater. 196 (2011) 173–179.
[12] Y. He, J. Zhang, H. Zhou, et al., Chem. Eng. J. 380 (2020) 122568.
[13] F. Ghanbari, M. Moradi, Chem. Eng. J. 310 (2017) 41–62.
[14] S.P. Rong, Y.B. Sun, Z.H. Zhao, Chin. Chem. Lett. 25 (2014) 187–192.
[15] B. Chen, Z. Liu, M. Zhang, et al., Plasma Sources Sci. Technol. 33 (2024) 11LT02.
[16] Z. Liu, M. Chen, D. Liu, High Voltage Eng. 48 (2022) 4196–4214.
[17] C.A. Aggelopoulos, S. Meropoulis, M. Hatzisymeon, et al., Chem. Eng. J. 398 (2020) 125622.
[18] Y. Cai, Y. Luo, B.C. Sun, et al., Chem. Eng. J. 377 (2019) 119897.
[19] J. Wu, Q. Xiong, J. Liang, et al., Chem. Eng. J. 384 (2020) 123300.
[20] S. Tang, D. Yuan, Y. Rao, et al., Chem. Eng. J. 337 (2018) 446–454.
[21] P. Lamichhane, T.R. Acharya, A. Jaiswal, et al., J. Environ. Chem. Eng. 12 (2024) 113445.
[22] B. Dojcinovic, B. Obradovic, M. Kuraica, et al., J. Serb. Chem. Soc. 81 (2016) 829–845.
[23] Q. Lin, G. Ni, Y. Jiang, et al., Plasma Sci. Technol. 16 (2014) 1036–1041.
[24] B. Wang, B. Dong, M. Xu, et al., Chem. Eng. Sci. 168 (2017) 90–100.
[25] I.M. Kolthoff, I.K. Miller, J. Am. Chem. Soc. 73 (1951) 3055–3059.
[26] S. Li, X. Cao, L. Liu, et al., Desalin. Water Treat. 53 (2015) 3018–3025.
[27] J. Ma, Y. Yang, X. Jiang, et al., Chemosphere 190 (2018) 296–306.
[28] E. Marotta, E. Ceriani, M. Schiorlin, et al., Water Res. 46 (2012) 6239–6246.
[29] P. Neta, R.E. Huie, A.B. Ross, J. Phys. Chem. Ref. Data 17 (1988) 1027–1284.
[30] X. Yang, P. Wu, W. Chu, et al., J. Water Process Eng. 43 (2021) 102231.
[31] Z. Liu, X. Li, H. Guo, et al., Chem. Eng. J. 507 (2025) 160480.
[32] Y. Huang, J. Zou, J. Lin, et al., Environ. Sci. Technol. 57 (2022) 18420–18432.
[33] D. Chen, Q. Bai, T. Ma, et al., Chem. Eng. J. 435 (2022) 134916.
[34] G. Yang, Y. Liang, Z. Xiong, et al., Chem. Eng. J. 425 (2021) 130689.
[35] B. Pang, Z. Liu, Y. Gao, et al., ACS Appl. Mater. Interfaces 17 (2024) 467–483.
[36] Z. Cai, X. Hao, X. Sun, et al., Water Res. 162 (2019) 369–382.